

## Fast computation of 3D Radon transform via a direct Fourier method

Salvatore Lanzavecchia and Pier Luigi Bellon

Dipartimento di Chimica Strutturale e Stereochimica Inorganica, Università degli Studi, via G. Venezian 21, 20133 Milano, Italy

Received on October 14, 1997; revised and accepted on November 21, 1997

### Abstract

**Motivation:** Arrays of three-dimensional (3D) data are ubiquitous in structural biology, biomedicine and clinical imaging. The Radon transform can be implied in their manipulation mainly for the solution of the inverse tomographic problem, since experimental data are often collected as projections or as samples of the Radon space. In electron tomography, new applications of the transform may become convenient if a fast and accurate transformation algorithm is adopted.

**Results:** A direct Fourier method (DFM) is proposed to compute the 3D Radon transform from a sampled function with compact support. This paper describes an already known two-step algorithm and illustrates its DFM implementation by coordinate transformations in 2D Fourier space. The algorithm is easily inverted to obtain a density distribution from the Radon transform. The main applications are in the field of electron tomography, especially in processes of angular refinement, since whatever projection of a structure can be retrieved from its Radon transform in a fast and accurate way. The times required to compute a number of projections with use of the Radon transform are compared with those required by other algorithms. Further uses of the Radon transform can be foreseen in applications based on 'projection onto convex sets' (POCS).

**Availability:** Software is available free of charge upon request to the authors.

**Contact:** salvator@csmtbo.mi.cnr.it

### Introduction

The Radon transform (Radon, 1917; 1986 for English translation) is an important item of integral geometry (Helgason, 1984) which holds the key for X-ray and emission tomography as well as for electron tomography (ET), radioastronomy and geophysics [Deans (1993) and references therein]. Besides this relevance in modern science, it offers an alternative way to represent and manipulate image and volume data, other than the usual pixel (Sanz *et al.*, 1988) or voxel representation (Radermacher, 1994).

The Radon transform  $\hat{f}$  can be defined for a suitable function  $f$  (see Appendix B in Deans, 1993), continuous and with compact support in an  $n$ -dimensional space. Its value in each point  $\mathbf{x}$  is obtained by integration over the  $(n - 1)$ -dimensional manifold orthogonal to  $\mathbf{x}$  in the function domain; in two dimensions (2D) the manifolds are lines, planes in 3D and so on. Thus, in an  $n$ -dimensional space, we have:

$$\hat{f}(p, \xi) = \int f(\mathbf{x}) \delta(p - \xi \cdot \mathbf{x}) d\mathbf{x},$$

$\xi$  being a unit vector in  $\mathbf{R}^n$ . In 3D,  $\hat{f}$  is conveniently represented in spherical coordinates  $(p, \nu, \varphi)$ ,  $p$  being the radial coordinate along  $\xi$  whose direction is described by two angular variables. A discrete version of  $\hat{f}$  is obtained by sampling the transform at equispaced values along  $p$ ,  $\nu$  and  $\varphi$ , although the sampling points are not equispaced in Euclidean space.

The Radon transform of a real object can be obtained experimentally, for instance, in an X-ray CT instrument. This is why a huge amount of literature is dedicated to recovering  $f$  from  $\hat{f}$ . Nowadays, different algorithms can satisfactorily solve this 'inverse problem'. In this paper, we wish to illustrate a fast and convenient algorithm to cope with the direct problem in 3D, i.e. obtaining the Radon transform of a sampled 3D density distribution. Some applications of computed Radon transforms will also be presented.

### Radon transform via Fourier transform

A tight relationship exists between Fourier transform (FT) and Radon transform of a function (Deans, 1993). The 1D FT of  $\hat{f}$  along the radial direction  $p$  represents a radial sampling of the  $n$ -dimensional FT of  $f$ . This fundamental property, based on the central section theorem, holds true in  $n$ -dimensional spaces. In 2D, it represents the basis for direct Fourier methods (DFM) to solve the inverse problem of X-ray CT (see, for example, Bellon and Lanzavecchia, 1997). Sampled versions of a 2D  $\hat{f}$ , called sinograms (see, for example, van Heel, 1987) can be computed either by projecting an image along a set of discrete directions (Bellon and Lanzavecchia, 1995) or by DFM (Lanzavecchia *et al.*, 1996). In the latter

case, the 2D FT of an image is converted from Cartesian to polar coordinates and  $\hat{f}$  is obtained by 1D FT inversion along  $p^*$ .

In 3D, the numerical computation of  $\hat{f}$  can again be performed in direct or in reciprocal space. In the former case, if  $f$  is sampled on a Cartesian grid, the direct computation of  $\hat{f}$  requires the interpolation of the density distribution on all planes, in order to make in-plane integration feasible. This involves a 3D interpolation in real space. In reciprocal space, 3D interpolation could be used to determine the complex coefficients along radial lines which are Fourier inverted; both processes are computation intensive.

The computing cost is substantially reduced in a two-step process. The simple recipe to carry it out is: first, rotate the structure stepwise around one axis and obtain a set of projections; second, compute the 2D Radon transform of each projection (Marr *et al.*, 1981). This method is easily understood since the projections obtained in the first step are collections of integrals of lines parallel to the projecting directions. In the second step, these line integrals are further integrated along all possible lines within the projection planes. The result of the two integrations corresponds to the plane integrals of  $f$ . The lay-out of these planes spans the domain of  $\hat{f}$  in spherical coordinates.

This two-step contrivance avoids the use of 3D interpolation; however, the computation of all projections in direct space is time expensive, especially if good accuracy is needed. The number of rotations required is half the number of independent projections needed (Bellon and Lanzavecchia, 1995). In what follows, a fast and accurate DFM implementation of the two-step algorithm is proposed.

### Fast DFM computation of the Radon transform

The collection of projections of a 3D structure on a set of planes rotated around a common axis is called a 'single-axis geometry' set. Suppose the structure is rotated stepwise around the  $z$  axis, with angular increments  $\Delta\upsilon$ , and projected on the  $x,z$  plane. The ordered set of projections is a 3D matrix sampling a continuous function  $P(r,z,\upsilon)$ . The planes parallel to  $z,\upsilon$  are the series of 2D Radon transforms (sinograms) of all structure sections orthogonal to  $z$ . Conversely, the single-axis geometry set can be obtained by computing the sinograms of all structure slices orthogonal to the rotation axis. Each slice, once copied and converted into a sinogram, can be stored back in the array which will eventually contain  $\hat{f}$ . In this way, the transposed matrix  $P(r,\upsilon,z)$  is obtained. Sinograms can be obtained efficiently as described elsewhere (Lanzavecchia *et al.*, 1996): the 2D FT of each slice is computed and converted to polar coordinates; 1D FT inversion along  $r^*$  yields the sinogram lines. Rotation axes other than  $z$  can be chosen if the proper transposition is performed first.

The second step is identical to the first one, provided that the array is transposed to  $P(r,z,\upsilon)$ . Now, each plane ( $\upsilon$  constant) contains a set of lines coming one from each sinogram. All planes are fetched in turn and their sinograms are computed as above to obtain the plane integrals, and stored back in the array which, at the end, contains  $f(p,\upsilon,\phi)$ . The process is represented schematically in Figure 1.

The DFM computation of sinograms performed in both steps can be inverted, with strictly comparable efficiency and accuracy, by carrying out sets of 2D tomographic reconstructions via DFM (see, for example, Bellon and Lanzavecchia, 1997). Thus, the 3D Radon transform is easily converted to the original structure.

### Interpolation in Fourier space

The conversion of coordinates requires a resampling in the complex Fourier space. This is possible since the Shannon criterion holds true in reciprocal space (Lanzavecchia and Bellon, 1998). Furthermore, for a function with a finite support, the relationship between a discrete Fourier series, evaluated with respect to the support, and the continuous transform is such that the coefficients of the former represent a discrete sampling of the latter (Brigham, 1974). In order to use the Shannon reconstruction, the band extension of the transform must be finite, though evaluating its extension might be difficult.

Our DFM to compute sinograms performs the resampling in Fourier domain with the moving window Shannon reconstruction algorithm (Lanzavecchia and Bellon, 1994) and with improved interpolating kernels (Lanzavecchia and Bellon, 1995). All interpolation steps in this study used a reconstructing function of the type:

$$\phi_n^A(x) = \frac{1}{n} \sum_{j=m}^{m+n-1} f(j/N) \frac{\sin[n \cdot \pi \cdot (x - j/N)]}{\sin[\pi \cdot (x - j/N)]} \cdot [\cos[\pi \cdot (x - j/N)]]^A$$

with a window width  $n = 11$  and  $A = 2$  ( $\phi_{11}^2$ ). Thus, each point of a polar raster is obtained from the linear combination of  $11 \times 11$  terms (real or imaginary) weighted by appropriate coefficients stored in tables to speed up computations.

### Applications to electron tomography

The reconstruction of a macromolecular protein assembly from its 2D projections observed in the electron microscope, which is the aim of ET, represents a fundamental tool of structural biology (Frank, 1996). Electron tomography is a typical inverse problem; its solution via the Radon transform has been proposed by Radermacher (1998). For ice-embedded samples, however, the directions along which the structure is projected are distributed at random. Thus, obtaining a regular sampling of the Radon space and inverting it to the real space by DFM is a cumbersome task. Rather, convol-

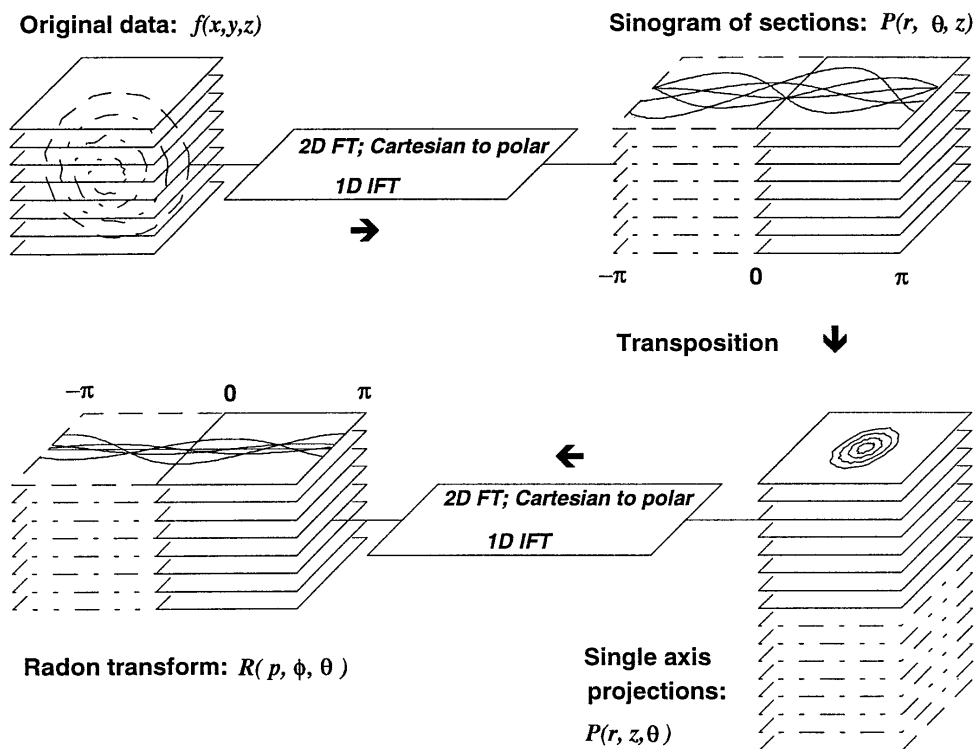


**Fig. 1.** Flow of operations in the two-step computation of the Radon transform  $R$  of a sampled function  $f$ . The dotted parts of arrays  $P$  and  $R$  are symmetry related to the parts enclosed by continuous lines and do not need to be computed. The process can be inverted, to obtain  $f$  from  $R$ , by reversing the flow direction.

uted back-projection methods (CBPM) are usually adopted in the reconstructions.

The Radon transform can play a role in ET refinement stages. Preliminary reconstructions are obtained from a number of observed projections assigned with a triad of Euler angles. Several strategies have been proposed to detect these angles (van Heel *et al.*, 1992; Radermacher, 1994; Penczek *et al.*, 1996). The first determinations are often inaccurate or completely wrong so that the projections need to be accurately aligned by an iterative process which starts from a preliminary structure; this ‘angular refinement’ (Schatz *et al.*, 1995) is a lengthy task. A ‘first trial’ reconstruction is projected along sets of angular values and the projections are compared with original images to assess their correspondence. Projections may be computed by: (i) straightforward integration of voxels using a nearest-neighbour (*n.n.*) approximation or bilinear interpolation (*b.i.*); both algorithms are quite inaccurate; (ii) by rotation of the array with a reliable interpolation (e.g. three-step algorithm with shifts in Fourier space; see Tosoni *et al.*, 1996), followed by discrete integration along the lines of the resulting array; (iii) by 3D interpolation in Fourier space (Malzbender, 1993); (iv) by extracting sinograms of projections from  $\hat{f}$  and reconstructing them. The latter technique, proposed by Radermacher

(1994), looks attractive since the Radon transform is easily obtained. The sinogram of a projection is recovered from  $\hat{f}$  with a process involving 2D interpolation on  $(v, \phi)$  planes, since each of its lines is parallel to  $p$ . Converting the sinogram into its parent projection is done by a DFM tomographic reconstruction (Lanzavecchia *et al.*, 1996).

We adopted this technique to refine random conical tilt reconstructions of metal replicas of some oligomers of the *Helicobacter pylori* toxin (Lanzavecchia *et al.* 1998). Preliminary reconstructions were projected to improve the azimuth angles estimated from correlation analysis of untilted micrographs (Radermacher *et al.*, 1987). The refinement required some iterations to converge. This experience offered the opportunity to compare the performances of some projecting algorithms for structures enclosed in  $64^3$  or  $128^3$  voxel boxes. Table 1a shows the times spent to compute Radon transforms; times to project structures with different algorithms are compared in Table 1b.

Accuracy is an important aspect in processes involving DFM. In the case of  $\hat{f}$  it can be evaluated by measuring how well a structure obtained after forward and back transformation compares with the original. Results of tests carried out on different structures show tiny errors, of no relevance in ET studies.

**Table 1.** (a) Times required to compute the direct Radon transform of a function and its inverse (IBM RISC 604e, 166 Mhz)

Operation	Array dimension		
	64 <sup>3</sup>	128 <sup>3</sup>	256 <sup>3</sup>
Direct			
Radon transform	8.5''	82''	782''
Inverse			
Radon transform	5''	50''	465''

(b) Times required to compute 128 projections of a structure with different methods. For projections obtained from the Radon transform, time is inclusive of transform computation; the method becomes more convenient on increasing the number of projections. Rotations are performed with a three-step algorithm and Fourier shift. Direct projections of volume use the nearest-neighbour technique (*n.n.*) or bilinear interpolation (*b.i.*). The same computer was used as in (a)

Method	Array dimension		
	64 <sup>3</sup>	128 <sup>3</sup>	256 <sup>3</sup>
Radon transform	18.5''	130''	1100''
Array rotation	170''	3220''	==
Direct			
projection <i>n.n.</i>	24''	200''	1613''
Direct			
projection <i>b.i.</i>	41''	340''	2830''

### Concluding remarks

Although Radon space is usually dealt with to solve the inverse problem, a fast algorithm to switch from direct to Radon space offers the opportunity to take advantage and to explore further the applications of this transform. Filtration algorithms, for instance, have been exploited to reject noise from sinograms (Karp *et al.*, 1988) and from a peculiar 3D projection space (Lanzavecchia and Bellon, 1996). A filter of this type can also be adopted in 3D Radon space.

Other possible applications deal with the recovery of missing data. This is the case of ET using conical and single-axis tilt geometry. The strategy of projection onto convex sets (POCS), devised for clinical tomography by Sezan and Stark (1984), has been introduced in ET by Carazo (Carazo and Carrascosa, 1987; Carazo, 1992). The technique is based on the idea that the reconstructed function and/or the data set must verify some general properties. If data are missing, the reconstruction fails to satisfy these properties, which can, however, be imposed as constraints. In this way, it is possible to recover missing information by an iterative process. Constraints can be devised and imposed on the set of experimental data in a projection space (Lanzavecchia and Bellon,

1996), but might also be imposed on 3D Radon space. A fast algorithm of direct and inverse Radon transform makes investigating further constraints in POCS applications attractive.

### Acknowledgements

This work has been financed by the Italian Ministry of University and Research (40% and 60%) and by the National Research Council of Italy.

### References

- Bellon, P.L. and Lanzavecchia, S. (1995) A direct Fourier method (DFM) for X-ray tomographic reconstructions and the accurate simulation of sinograms. *Int. J. Bio-Med. Comp.*, **38**, 55–69.
- Bellon, P.L. and Lanzavecchia, S. (1997) Fast direct Fourier methods, based on 1- and 2-pass coordinates transformation, yields accurate reconstructions of X-ray CT clinical images. *Phys. Med. Biol.*, **42**, 443–463.
- Brigham, O.E. (1974) *The Fast Fourier Transform*. Prentice-Hall, Englewood Cliffs, NJ.
- Carazo, J.M. (1992) The fidelity of 3D reconstructions from incomplete data and the use of restoration methods. In Frank, J. (ed.), *Electron Tomography*. Plenum Press, New York, pp. 117–164.
- Carazo, J.M. and Carrascosa, J.L. (1987) Information recovery in missing angular cases: an approach by convex projections method in three dimensions. *J. Microsc.*, **145**, 23–43.
- Deans, S.R. (1993) *The Radon Transform and Some of its Applications*. Krieger Publishing, Malabar, FL.
- Frank, J. (1996) *Three-Dimensional Electron Microscopy of Macromolecular Assemblies*. Academic Press, New York.
- Helgason, S. (1984) *Groups and Geometric Analysis*. Academic Press, New York.
- Karp, J.S., Muehlechner, G. and Lewitt, R.M. (1988) Constrained Fourier space method for compensation of missing data in emission computed tomography. *IEEE Trans. Med. Imaging*, **7**, 21–25.
- Lanzavecchia, S. and Bellon, P.L. (1994) A moving window Shannon reconstruction for image interpolation. *J. Vis. Commun. Image Repres.*, **5**, 255–264.
- Lanzavecchia, S. and Bellon, P.L. (1995) A bevy of novel interpolating kernel for the Shannon reconstruction of high band pass images. *J. Vis. Commun. Image Repres.*, **6**, 122–131.
- Lanzavecchia, S. and Bellon, P.L. (1996) Electron tomography in conical tilt geometry: the accuracy of a direct Fourier method (DFM) and the suppression of non tomographic noise. *Ultramicroscopy*, **63**, 247–261.
- Lanzavecchia, S. and Bellon, P.L. (1998) The moving window Shannon reconstruction in direct and Fourier domain: application in tomography. *Scanning Microsc.*, in press.
- Lanzavecchia, S., Bellon, P.L., Lupetti, P., Dallai, R., Rappuoli, R. and Telford, J.L. (1998) Three dimensional reconstruction of metal replicas of the *H. pylori* vacuolating cytotoxin. *J. Struct. Biol.*, **121**, in press.
- Lanzavecchia, S., Tosoni, L. and Bellon, P.L. (1996) Fast sinogram computation and the sinogram-based alignment of images. *Comput. Applic. Biosci.*, **12**, 531–537.

- Malzbender,T. (1993) Fourier volume rendering. *ACM Trans. Graph.*, **12**, 233–250.
- Marr,R.B., Chen,C. and Lauterbur,P.C. (1981) On two approaches to 3D reconstruction in NMR zeugmatography. In Herman,G.T. and Natterer,F. (eds), *Mathematical Aspects of Computerized Tomography*. Springer Verlag, New York, pp. 225–240.
- Penczek,P.A., Zhu,J. and Frank,J. (1996) A common-lines based method for determining orientations for  $N>3$  particle projections simultaneously. *Ultramicroscopy*, **63**, 205–218.
- Radermacher,M. (1994) Three-dimensional reconstruction from random projections: orientational alignment via Radon transforms. *Ultramicroscopy*, **53**, 121–136.
- Radermacher,M. (1998) Radon transform technique for alignment and 3D-reconstruction from random projections. *Scanning Microsc.*, in press.
- Radermacher,M., Wagenknecht,T., Verschoor,A. and Frank,J. (1987) Three-dimensional reconstruction from a single-exposure, random conical tilt series applied to the 50S ribosomal subunit of *Escherichia coli*. *J. Microsc.*, **146**, 113–136.
- Radon,J. (1917) Über die Bestimmung von Funktionen durch ihre Integralwerte längs gewisser Mannigfaltigkeiten. Berichte über die Verhandlungen der Königlich Sächsischen Gesellschaft der Wissenschaften zu Leipzig. *Math. Phys. Klasse*, **69**, 262–277.
- Radon,J. (1986) On the determination of functions from their integral values along certain manifolds. *IEEE Trans. Med. Imaging*, **5**, 170–176.
- Sanz,J.L.C., Hinkle,E.B. and Jain,A.K. (1988) *Radon and Projection Transform-Based Computer Vision*. Springer-Verlag, Berlin.
- Schatz,M., Orlova,E.V., Dube,P., Jäger,J. and van Heel,M. (1995) Structure of *Lumbricus terrestris* hemoglobin at 30 Å resolution determined using angular reconstitution. *J. Struct. Biol.*, **114**, 28–40.
- Sezan,M.I. and Stark,H. (1984) Tomographic image reconstruction from incomplete view data by convex projections and direct Fourier inversion. *IEEE Trans. Med. Imaging*, **3**, 91–98.
- Tosoni,L., Lanzavecchia,S. and Bellon,P.L (1996) Image and volume data rotation with 1- and 3-pass algorithms. *Comput. Applic. Biosci.*, **12**, 549–552.
- van Heel,M. (1987) Angular reconstitution: a posteriori assignment of projection directions for 3D reconstruction. *Ultramicroscopy*, **21**, 111–124.
- van Heel,M., Winkler,H.P., Orlova,E.V. and Schatz,M. (1992) Structure analysis of ice-embedded single particles. *Scanning Microsc. Suppl.*, **6**, 23–42.